

Journal of Materials Chemistry C

Accepted Manuscript



This is an *Accepted Manuscript*, which has been through the Royal Society of Chemistry peer review process and has been accepted for publication.

Accepted Manuscripts are published online shortly after acceptance, before technical editing, formatting and proof reading. Using this free service, authors can make their results available to the community, in citable form, before we publish the edited article. We will replace this *Accepted Manuscript* with the edited and formatted *Advance Article* as soon as it is available.

You can find more information about *Accepted Manuscripts* in the [Information for Authors](#).

Please note that technical editing may introduce minor changes to the text and/or graphics, which may alter content. The journal's standard [Terms & Conditions](#) and the [Ethical guidelines](#) still apply. In no event shall the Royal Society of Chemistry be held responsible for any errors or omissions in this *Accepted Manuscript* or any consequences arising from the use of any information it contains.

Cite this: DOI: 10.1039/c0xx00000x

PAPER

www.rsc.org/xxxxxx

Intense Electroluminescence from ZnO Nanowires

Xun Yang,^{a,b} Chong-Xin Shan,^{a,c,*} Ming-Ming Jiang,^a Jie-Ming Qin,^{d,e} Guang-Chong Hu,^{a,b} Shuang-Peng Wang,^a Hong-An Ma,^f Xiao-Peng Jia,^f De-Zhen Shen^{a,*}

Received (in XXX, XXX) Xth XXXXXXXXXX 20XX, Accepted Xth XXXXXXXXXX 20XX

DOI: 10.1039/b000000x

Vertically aligned ZnO nanowires have been prepared, and intense electroluminescence (EL) has been observed with holes injected into the nanowires from *p*-type ZnO prepared via a high pressure high temperature route. The emission can be attributed to the radiative recombination between the electrons in the nanowires and the injected holes, and the power of the EL can reach about 10 μ W when the injection current is 20 mA. The intense emission is believed to be resulted from both the relatively high quality of the nanowires and the holes injection from the *p*-type ZnO.

Introduction

Zinc oxide (ZnO) has long been considered as a promising candidate for efficient ultraviolet (UV) light-emitting devices (LEDs) and low-threshold lasers due to its wide bandgap and large exciton binding energy.¹⁻¹⁴ However, although numerous efforts have been paid, the performance of ZnO LEDs is still far below expectation. It is accepted that to realize efficient electroluminescence (EL), both high quality active layer and efficient carrier injection are necessary. For the high quality active layer, self-assembled nanostructures usually have relatively high crystalline and optical quality. Considering that one of the most unique characters of ZnO lies in its rich nanostructures,^{4,15-17} if the nanostructures can be employed as the active layer, efficient EL from ZnO may be expected. Carrier injection is another necessity for efficient EL. It is known that ZnO is intrinsically an *n*-type semiconductor,¹⁸ which means that there are many electrons, but holes are rare in this material. A natural way to achieve hole dominant conduction in ZnO is doping. However, the *p*-type doping of ZnO has long been a challenging issue although numerous efforts have been paid.¹⁹⁻²³ Many methods including molecular beam epitaxy, metalorganic chemical vapor deposition, magnetron sputtering, pulsed laser deposition, etc.,²⁴⁻²⁷ have been adopted for the *p*-type doping of ZnO. However, this challenging issue has not been resolved yet, and *p*-type doping is still a huge barrier that hinders the realization of ZnO based LEDs. Note that the above methods employed for the *p*-type doping of ZnO is usually running at moderate temperature and pressure. It is known that temperature and pressure are two important parameters that determine the

thermal dynamics in the growth process of a material, so if high pressure high temperature can be adopted for the *p*-type doping of ZnO, the growth dynamic during the doping process may be altered, and surprising results may be attained. Actually, low-resistivity *p*-type ZnO with good stability and reproducibility has been prepared in a high pressure high temperature route.²⁸ Nevertheless, none report on LEDs using the *p*-type ZnO fabricated via such route can be found up to now, which casts a shadow whether the *p*-type ZnO prepared via this route can be applied in optoelectronic devices.

In this paper, we show that by employing high quality ZnO nanowires as the active layer of a LED, with holes injected from *p*-type ZnO prepared in a high pressure high temperature route. Intense emission can be achieved, and the power of the emission can reach 10 μ W when the injection current is 20 mA, which is amongst the best values ever reported for ZnO-based LEDs.²¹ The emission is believed to originate from the radiative recombination of the injected holes and the electrons in the ZnO nanowires.

Experimental

The ZnO nanowires were fabricated on *a*-plane sapphire in a metalorganic chemical vapor deposition technique. The precursors used for the growth of the nanowires are diethylezinc and oxygen, and high-purity (9 N) nitrogen was employed as the carrier gas to lead the precursors into the growth chamber. Prior to the growth, the substrates were pretreated at 700 °C under 3.1×10^{-3} Pa for 30 min to remove the absorbed contaminants on the substrate surface. During the growth process, the substrate temperature was kept at 700 °C and the pressure in the chamber at 3000 Pa. The *p*-type ZnO employed as the hole source of the LEDs was prepared via a high temperature high pressure method. 99.99% ZnO powder and 99.99% Sb₂O₃ powder was mixed together uniformly, and the mole ratio of Sb₂O₃ to ZnO is 1:19. The mixture was pressed into a disk with a diameter of 13 mm and a height of 5 mm under 0.5 GPa, then the disk was put into a Mo ampoule to be sintered isothermally for 15 min under 5 GPa at 1450 °C. After that, the surface layer of both sides of the disk were removed to avoid any diffusion of impurities into the sample. When the preparation of the nanowires and the ZnO:Sb is finished, an indium layer was deposited onto the ZnO:Sb and the

ZnO nanowires acting as electrodes in a thermal evaporation method. Then the ZnO:Sb was bonded together with the nanowires by a clip to form the ZnO:Sb/*n*-ZnO nanowire structures.

The morphology and crystalline quality of the ZnO nanowires was characterized using a Hitachi S4800 field emission scanning electron microscope (SEM) and a FEI Tecnai F20 transmission electron microscope (TEM). The structural properties of the nanowires and the ZnO:Sb were assessed by a Bruke D8 x-ray diffractometer (XRD). The photoluminescence (PL) spectra of the nanowires and ZnO:Sb were measured using a spectrometer employing the 325 nm line of a He-Cd laser as the excitation source. The electrical properties of the ZnO:Sb were measured in a Lakeshore 7707 Hall measurement system. The Sb concentration in the ZnO:Sb was determined by energy-dispersive X-ray spectroscopy (EDS). Current-voltage (*I*-*V*) characteristics of the ZnO:Sb/*n*-ZnO nanowire structures were studied by a Agilent B1500A semiconductor device analyzer. Electroluminescence (EL) measurement of the structures was carried out in a Hitachi F4500 spectrometer with a continuous current power source, and the output power of the LEDs was recorded using an OPHIR Nova II power meter. The electrical potential distribution and carrier distribution in the ZnO:Sb/*n*-ZnO nanowire structures have been simulated using a finite difference time domain (FDTD) method.

Results and discussion

The morphology of the ZnO nanowires is shown in Figs. 1a and 1b. From the plan-view SEM image in Fig. 1a and the cross-sectional image in Fig. 1b, one can see that the ZnO nanowires were grown vertically on the substrate, and the nanowires are about 50 nm in diameter and 900 nm in length. Fig. 1c shows a typical TEM image of the ZnO nanowires, one can see that the nanowires show smooth surface, symbolizing the well-crystalline of the nanowires. High resolution TEM image taken from an individual nanowire is shown in Fig. 1d. The image shows well-resolved lattice fringes, and the distance between two adjacent planes is around 0.26 nm, confirming *c*-axis growth direction and high crystalline quality of the nanowires.

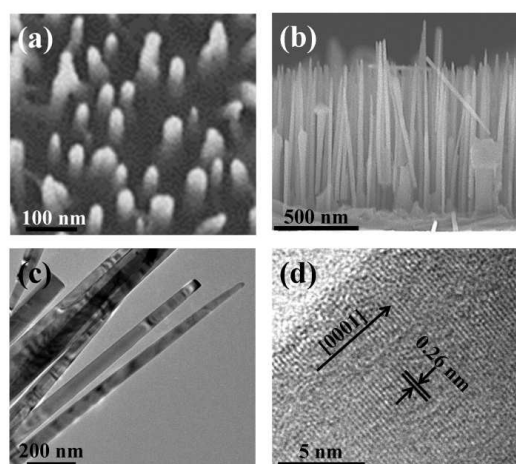


Fig. 1. Plan-view (a) and cross-sectional (b) SEM image of the ZnO nanowires; (c) TEM image of the ZnO nanowires; (d) High resolution TEM image of an individual nanowire.

Fig. 2a shows the XRD pattern of the ZnO nanowires, besides the diffraction from the sapphire substrate, only two peaks at 34.44° and 72.54° can be observed, which can be attributed to the diffraction from the (002) and (004) facet of wurtzite ZnO, respectively. The insert of Fig. 2a illustrates the x-ray rocking curve of the nanowires, and the curve shows a Gaussian shape with a full-width half-maximum (FWHM) of around 0.59°. To assess the optical quality of the ZnO nanowires, temperature-dependent PL spectra from 90 K to 300 K were recorded, as shown in Fig. 2b. The 90 K PL spectrum shows four peaks at around 3.237 eV, 3.313 eV, 3.356 eV and 3.370 eV. Among these peaks, the dominant one at 3.370 eV can be attributed to the free exciton (FX_A) emission of ZnO.²⁹ There also appears a shoulder at around 3.381 eV, which can be attributed to the emission of B-excitons in ZnO.²⁹ According to their positions, the peaks at 3.356 eV and 3.313 eV can be attributed to the emission from donor-bound exciton (D⁰X) and donor-acceptor pairs (DAP).^{29,30} The peak at 3.237 eV has an energy difference of 76 meV with the DAP emission, which is close to the phonon energy of ZnO (72 meV),²⁹ thus this peak may be the phonon replica of DAP.³⁰ Although free exciton emission has been frequently observed in the low-temperature PL spectra of ZnO film and nanostructures, it is usually weak and the spectrum is usually dominated by emissions from excitons localized by impurities.²⁹⁻³¹ The dominant free exciton emission at 90 K and the appearance of B-exciton emission in our case reveals the high optical quality of the ZnO nanowires, which lay a solid ground for the intense emission obtained from the nanowires.

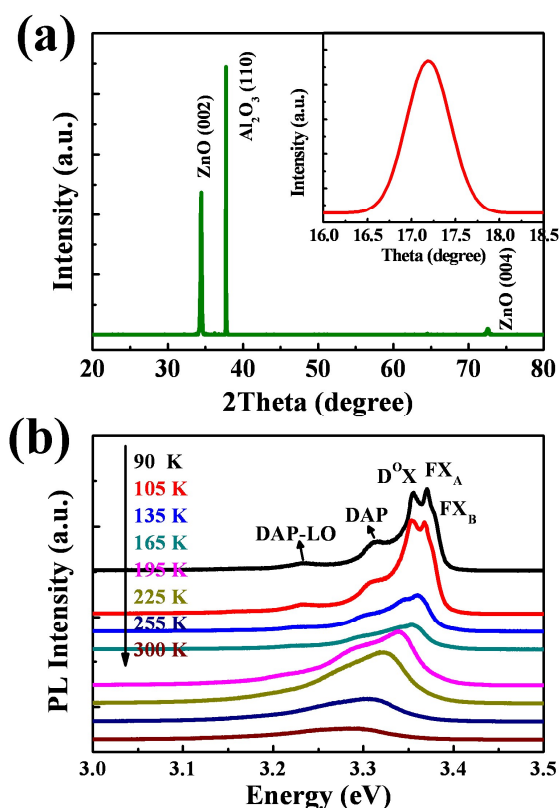


Fig. 2. (a) XRD pattern of the ZnO nanowires, and the inset shows the x-ray rocking curve of the ZnO nanowires; (b) temperature-dependent PL spectra of the ZnO nanowires.

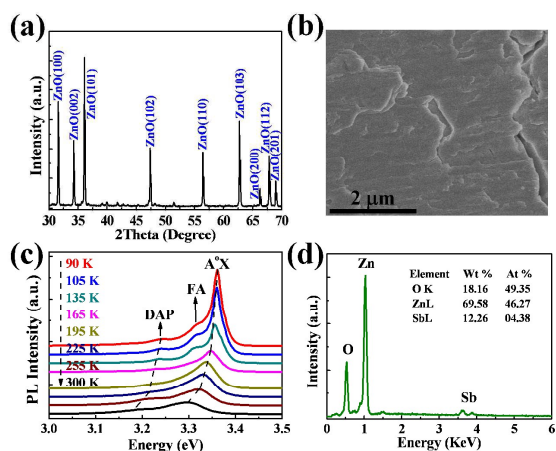


Fig. 3. XRD pattern (a); SEM image (b); temperature-dependent PL spectra (c), and EDS spectrum (d) of the ZnO:Sb sample.

The XRD pattern of the ZnO:Sb is shown in Fig. 3a. All the prominent peaks can be attributed to the diffraction from wurtzite ZnO, while the weak peaks from Sb₂O₅. Note that all the peaks from the ZnO:Sb shift to smaller angle side compared with the standard peaks of ZnO, which symbolizes that Sb has been incorporated into lattice of ZnO considering that the radius of Sb³⁺ (0.76 Å) is larger than that of Zn²⁺ (0.74 Å). Also the appearance of Sb₂O₅ related peaks indicates that some of the Sb₂O₅ may separate out from the ZnO matrix. The morphology of the ZnO:Sb is shown in Fig. 3b, and one can see that dense layer has been formed in the ZnO:Sb. Temperature-dependent PL measurements from 90 to 300 K are also performed to investigate the optical properties of the ZnO:Sb, as shown in Fig. 3c. From the 90 K PL spectrum, three peaks can be observed at 3.361 eV, 3.316 eV, and 3.241 eV, respectively. The 3.361 eV and 3.316 eV peaks are ascribed to neutral acceptor bound exciton (A⁰X) and electron transition from conduction band to acceptor level (FA).^{28,32,33} The peak at 3.241 eV can be attributed to the DAP emission.^{32,33} With the rise of temperature, the FA emission disappears gradually, while the A⁰X and DAP emissions can be observed from the 300 K PL spectrum at 3.288 eV (377 nm) and 3.198 eV (388 nm), respectively. The EDS spectrum of the ZnO:Sb is shown in Fig. 3d, from which only the signals from Zn, O and Sb can be observed, and the Sb content in the ZnO:Sb is about 4.38 atom%, in rough agreement with the mole ration of Sb₂O₅ to ZnO in the precursors (1: 19).

To act as the hole source for the ZnO nanowires, the ZnO:Sb should have relatively high hole concentration. To assess the hole concentration of the ZnO:Sb, Hall measurement has been carried out. It is revealed that the ZnO:Sb behaviors *p*-type conduction, with the room temperature hole concentration and Hall mobility of $3.8 \times 10^{19} \text{ cm}^{-3}$ and $1.9 \text{ cm}^2 \text{ V}^{-1} \text{ s}^{-1}$, respectively. Similar results have been reported previously,²⁸ and the origin of the *p*-type conductivity in ZnO:Sb is usually attributed to the formation of Sb_{Zn}-2V_{Zn} complexes.³⁴ Such a high hole concentration is favorable for acting as a hole source.

To inject holes into the ZnO nanowires, the *p*-ZnO:Sb has been bonded together with the ZnO nanowires by a clip to form the *p*-ZnO:Sb/*n*-ZnO nanowire structures. Fig. 4a shows the schematic illustration of the structure. The structure exhibits an obvious rectifying characteristic with a turn-on voltage of about

4.6 V, as shown in Fig. 4b. The insert of Fig. 4b shows the *I*-*V* curves for In contact on *p*-ZnO:Sb and *n*-ZnO nanowires. The linear curves reveal that ohmic contacts have been obtained in both cases, indicating the rectifying effect comes from *p*-*n* junctions formed between the *p*-ZnO:Sb and the *n*-ZnO nanowires.

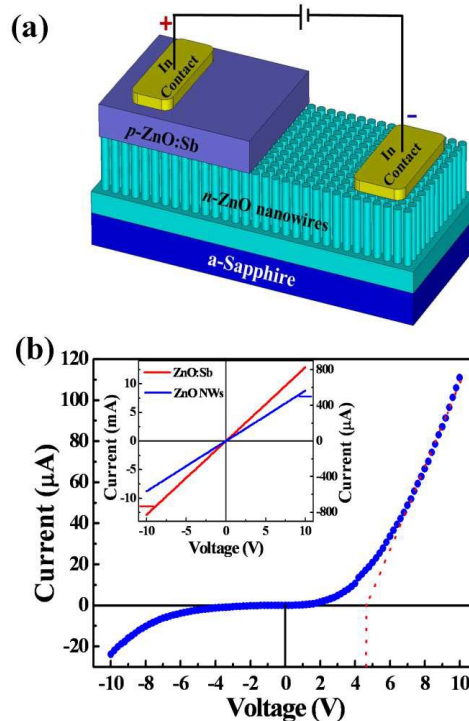


Fig. 4. (a) Schematic illustration of the *p*-ZnO:Sb/*n*-ZnO nanowire structure; (b) *I*-*V* curve of the *p*-ZnO:Sb/*n*-ZnO nanowire structure, the inset shows the *I*-*V* curves of the In contact on the *n*-ZnO nanowires and the *p*-ZnO:Sb.

To test the application of the structure in LEDs, a forward bias has been applied onto the structure, and purple emission can be observed clearly, as indicated in Fig. 5. Fig. 5a shows the a typical optical image of the device, and the output power can reach 10 μW when the injection current is 20 mA (with a bias voltage of around 85 V), which is amongst the highest values ever reported for ZnO-based LEDs.^{21,35} Error! Bookmark not defined. The EL spectra of the device are shown in Fig. 5b. There is a dominant emission band at around 396 nm, and another weak emission at around 500 nm is also visible. The dominant emission can be attributed to the NBE emission, while the weak one to the deep-level related emission of ZnO.

To explore the origin of the EL emission, the room temperature PL spectra of the ZnO nanowires and ZnO:Sb has been measured, as shown in Fig. 5c. It can be found that the PL spectrum of the ZnO nanowires shows a strong peak at around 377 nm, while the deep-level emission is almost undetectable. Nevertheless, the spectrum of the *p*-ZnO:Sb sample is dominated by the deep-level related emission of ZnO, while the NBE emission of ZnO is weak. Note that there appear two peaks for the NBE emission of the ZnO:Sb, and the peak at 377 nm can be attributed to the acceptor bounded excitonic emission of ZnO,

and the shoulder at 388 nm is from the DAP emission based on the temperature dependent PL spectra shown in Fig. 3c. One can see from Fig. 5 that the EL spectra of the p -ZnO:Sb/ n -ZnO nanowire structure is similar in shape with the PL spectrum of the ZnO nanowires although the peak position is slightly different, thus the EL emission in the structure may come from the radiative recombination of electrons and holes in the ZnO nanowires.

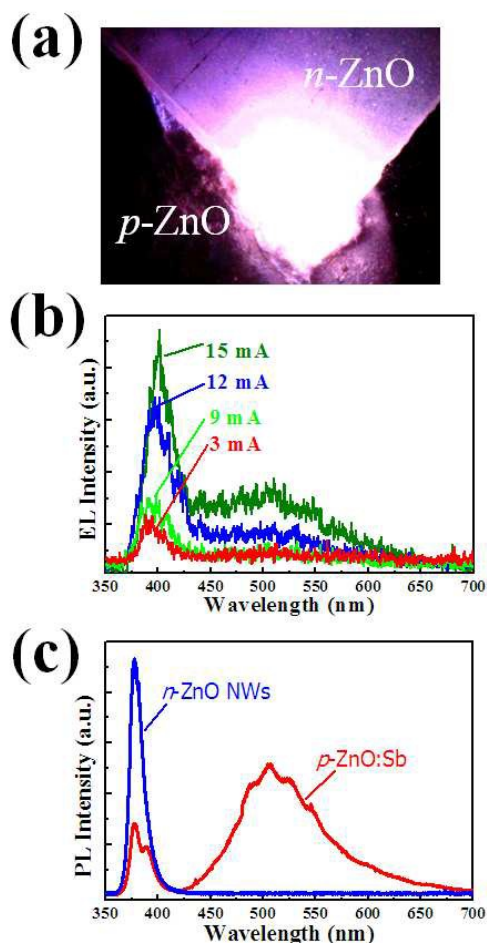


Fig. 5. Optical image (a) and EL spectra (b) of the p -ZnO:Sb/ n -ZnO nanowire structure; (c) room temperature PL spectra of the n -ZnO nanowires and p -ZnO:Sb.

In order to understand the emission mechanism of the p -ZnO:Sb/ n -ZnO nanowire structures better, the distribution of charge carriers and electric potential in the p -ZnO:Sb/ n -ZnO structure under forward bias has been simulated using the FDTD method, as illustrated in Fig. 6. In the p -ZnO:Sb/ n -ZnO nanowire structures, since the hole concentration of the ZnO:Sb ($3.8 \times 10^{19} \text{ cm}^{-3}$) is much higher than the electron concentration in the nanowires (usually in the order of 10^{16} cm^{-3}), the depletion area of the p - n junction will be distributed mainly in the nanowires, as indicated in Fig. 6a. The carrier distribution in the p -ZnO:Sb/ n -ZnO nanowire structure is shown in Fig. 6b, one can see that the holes in the p -ZnO:Sb can be injected into the ZnO nanowires. Therefore, the injected holes will recombine with the electrons in the ZnO nanowires, and electroluminescence from the ZnO

nanowires will be detected. The relatively high structural and optical quality of the nanowires may facilitate the occurrence of near ultraviolet emission. As for the slightly redshift of the EL position compared with the NBE emission of ZnO, it may come from the heating effect caused by the injection of continuous current. Note that none reports on ZnO LEDs p -type ZnO prepared via high pressure high temperature method has demonstrated before.

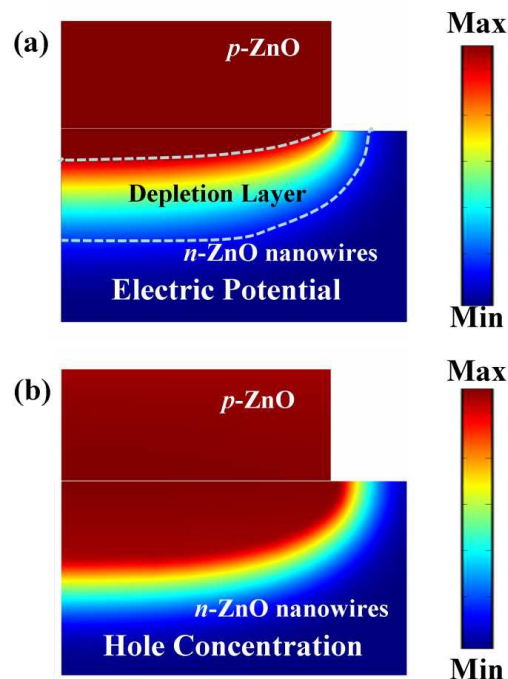


Fig. 6. Spatial distribution of the electric potential (a) and holes concentration (b) in the p -ZnO:Sb/ n -ZnO nanowire structure.

Conclusions

In summary, ZnO nanowires have been prepared, and with holes injected from p -ZnO:Sb fabricated via a high pressure and high temperature route, bright emission has been observed. The output power can reach around $10 \mu\text{W}$ when the injection current is 20 mA, which is amongst the best values ever reported for ZnO LEDs. The intense emission can be attributed to the relative high structural and optical quality of the nanowires and the relatively high hole concentration of the ZnO:Sb layer. The results reported here may provide a facile route to high performance ZnO electroluminescence.

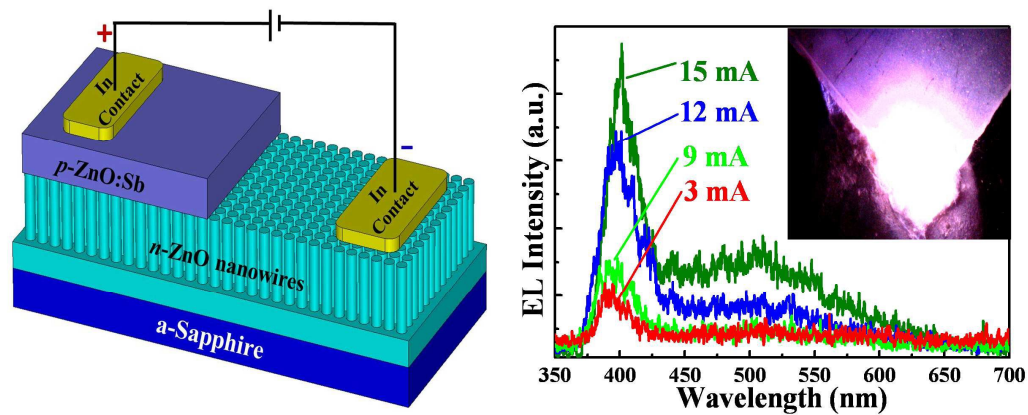
Acknowledgement

This work is financially supported by the National Basic Research Program of China (2011CB302005), the National Science Foundation for Distinguished Young Scholars of China (61425021), the Natural Science Foundation of China (11134009, 11404328, 11374296, 11464035 and 61177040), and the Science and Technology Developing Project of Jilin Province (20111801 and 20140101052JC).

Notes and references

- ^a State Key Laboratory of Luminescence and Applications, Changchun Institute of Optics, Fine Mechanics and Physics, Chinese Academy of Sciences, Changchun 130033, China.
- ^b University of Chinese Academy of Sciences, Beijing 100049, China.
- ^c School of Physical Engineering, Zhengzhou University, 450052, China.
- ^d School of Materials Science and Engineering, Changchun University of Science and Technology, Changchun 130022, China.
- ^e School of Physics, Inner Mongolia University for Nationalities, Tongliao 028000, China.
- ^f State Key Laboratory of Superhard Materials, Jilin University, Changchun 130012, China.
- 1 H. Zhu, C. X. Shan, B. Yao, B. H. Li, J. Y. Zhang, Z. Z. Zhang, D. X. Zhao, D. Z. Shen, X. W. Fan, Y. M. Lu and Z. K. Tang, *Adv. Mater.*, 2009, **21**, 1613.
 - 2 G. Y. Zhu, C. X. Xu, L. S. Cai, J. T. Li, Z. L. Shi, Y. Lin, G. F. Chen, T. Ding, Z. S. Tian and J. Dai, *ACS Appl. Mater. Interfaces*, 2012, **4**, 6195-6201.
 - 3 P. N. Ni, C. X. Shan, S. P. Wang, X. Y. Liu and D. Z. Shen, *J. Mater. Chem. C*, 2013, **1**, 4445-4449.
 - 4 H. X. Dong, Y. Liu, J. Lu, Chen, J. Wang and L. Zhang, *J. Mater. Chem. C*, 2013, **1**, 202-206.
 - 5 J. Huang, S. Chu, J. Y. Kong, L. Zhang, C. M. Schwarz, G. P. Wang, L. Chernyak, Z. H. Chen and J. L. Liu, *Adv. Opt. Mater.*, 2013, **1**, 179-185.
 - 6 G. Lozano, D. J. Louwers, S. R. K. Rodriguez, S. Murai, O. T. Jansen, M. A. Verschuuren and J. G. Rivas, *Light: Sci. Appl.*, 2013, **2**, e66.
 - 7 Q. Qiao, C. X. Shan, J. Zheng, H. Zhu, S. F. Yu, B. H. Li, Y. Jia and D. Z. Shen, *Nanoscale*, 2013, **5**, 513-517.
 - 8 X. Y. Liu, C. X. Shan, S. P. Wang, H. F. Zhao and D. Z. Shen, *Nanoscale*, 2013, **5**, 7746-7749.
 - 9 H. Zhu, C. X. Shan, B. Yao, B. H. Li, J. Y. Zhang, Z. Z. Zhang, D. X. Zhao, D. Z. Shen, X. W. Fan, Y. M. Lu and Z. K. Tang, *Adv. Mater.*, 2009, **21**, 1613-1617.
 - 10 X. Z. Zhang, X. J. Zhang, J. B. Xu, X. D. Shan, J. Xu and D. P. Yu, *Opt. Lett.*, 2009, **34**, 2533-2535.
 - 11 X. M. Mo, G. J. Fang, H. Long, S. Z. Li, H. H. Huang, H. N. Wang, Y. H. Liu, X. Q. Meng, Y. P. Zhang and C. X. Pan, *J. Lumin.*, 2013, **137**, 116-120.
 - 12 S. Z. Li, W. W. Lin, G. J. Fang, F. Huang, H. H. Huang, H. Long, X. M. Mo, H. N. Wang, W. J. Guan and X. Z. Zhao, *J. Lumin.*, 2013, **140**, 110-113.
 - 13 X. M. Mo, G. J. Fang, H. Long, S. Z. Li, H. N. Wang, Z. Chen, H. H. Huang, W. Zeng, Y. P. Zhang and C. X. Pan, *Phys. Chem. Chem. Phys.*, 2014, **16**, 9302-9308.
 - 14 Y. Yang, X. W. Sun, B. K. Tay, G. F. You, S. T. Tan and K. L. Teo, *Appl. Phys. Lett.*, 2008, **93**, 253107.
 - 15 K. Mahmood, S. B. Park and H. J. Sung, *J. Mater. Chem. C*, 2013, **1**, 3138-3149.
 - 16 C. K. Xu, P. Shin, L. L. Cao and D. Gao, *J. Phys. Chem. C*, 2010, **114**, 125-129.
 - 17 H. M. Cheng, W. H. Chiu, C. H. Lee, S. Y. Tsai and W. F. Hsieh, *J. Phys. Chem. C*, 2008, **112**, 16359-16364.
 - 18 S. B. Zhang, S. H. Wei and A. Zunger, *Phys. Rev. B*, 2001, **63**, 075205.
 - 19 S. J. Jiao, Z. Z. Zhang, Y. M. Lu, D. Z. Shen, Y. Yao, J. Y. Zhang, B. H. Li, D. X. Zhao, X. W. Fan and Z. K. Tang, *Appl. Phys. Lett.*, 2006, **88**, 031911.
 - 20 A. Tsukazaki, A. Ohtomo, T. Onuma, M. Ohtani, T. Makino, M. Sumiya, K. Ohtani, S. F. Chichibu, S. Fuke, Y. Segawa, H. Ohno, H. Koinuma and M. Kawasaki, *Nature Mater.*, 2005, **4**, 42-46.
 - 21 K. Nakahara, S. Akasaka, H. Yuji, K. Tamura, T. Fujii, Y. Nishimoto, D. Takamizu, A. Sasaki, T. Tanabe, H. Takasu, H. Amai, T. Onuma, S. F. Chichibu, A. Tsukazaki, A. Ohtomo and M. Kawasaki, *Appl. Phys. Lett.*, 2010, **97**, 013501.
 - 22 J. C. Fan, C. Y. Zhu, S. Fung, Y. C. Zhong, K. S. Wong, Z. Xie, G. Brauer, W. Anwand, W. Skorupa, C. K. To, B. Yang, C. D. Belling and C. C. Ling, *J. Appl. Phys.*, 2009, **106**, 073709.
 - 23 H. Shen, C. X. Shan, J. S. Liu, B. H. Li, Z. Z. Zhang and D. Z. Shen, *Phys. Status Solidi B*, 2013, **250**, 2102-2105.
 - 24 D. C. Look, D. C. Reynolds, C. W. Litton, R. L. Jones, D. B. Eason and G. Cantwell, *Appl. Phys. Lett.*, 2002, **81**, 1830-1832.
 - 25 Y. Ma, G. T. Du, S. R. Yang, Z. T. Li, B. J. Zhao, X. T. Yang, T. P. Yang, Y. T. Zhang and D. L. Liu, *J. Appl. Phys.*, 2004, **95**, 6268-6272.
 - 26 Y. J. Zeng, Z. Z. Ye, W. Z. Xu, D. Y. Li, J. G. Lu, L. P. Zhu and B. H. Zhao, *Appl. Phys. Lett.*, 2006, **88**, 062107.
 - 27 M. S. Oh, S. H. Kim and T. Y. Seong, *Appl. Phys. Lett.*, 2005, **87**, 122103.
 - 28 J. M. Qin, B. Yao, Y. Yan, J. Y. Zhang, X. P. Jia, Z. Z. Zhang, B. H. Li, C. X. Shan and D. Z. Shen, *Appl. Phys. Lett.*, 2009, **95**, 022101.
 - 29 J. N. Dai, H. C. Liu, W. Q. Fang, L. Wang, Y. Pu, Y. F. Chen and F. Y. Jiang, *J. Cryst. Growth*, 2005, **283**, 93-99.
 - 30 C. X. Shan, Z. Liu and S. K. Hark, *Phys. Lett.*, 2008, **92**, 073103.
 - 31 S. S. Kurbanov, H. D. Cho and T. W. Kang, *Opt. Commun.*, 2011, **284**, 240-244.
 - 32 F. X. Xiu, Z. Yang, L. J. Mandalapu, D. T. Zhao and J. L. Liu, *Appl. Phys. Lett.*, 2005, **87**, 252102.
 - 33 X. Fang, J. H. Li, D. X. Zhao, B. H. Li, Z. Z. Zhang, D. Z. Shen, X. H. Wang and Z. P. Wei, *Thin Solid Films*, 2010, **518**, 5687-5689.
 - 34 S. Limpijumnon, S. B. Zhang, S. H. Wei and C. H. Park, *Phys. Rev. Lett.*, 2004, **92**, 155504.
 - 35 H. Kato, T. Yamamuro, A. Ogawa, C. Kyotani and M. Sano, *Appl. Phys. Express*, 2011, **4**, 091105.

Graphic Abstract



Intense electroluminescence has been obtained from ZnO nanowires with holes injected from *p*-ZnO:Sb prepared via high pressure high temperature method.